INDUCED HORIZONTAL STRESS METHOD OF PILLAR DESIGN IN OIL SHALE

J.F.T. Agapito
J.F.T. Agapito and Associates, Inc.
715 Horizon Drive, Suite 340
Grand Junction, Colorado 81501

M.P. Hardy
J.F.T. Agapito and Associates, Inc.
715 Horizon Drive, Suite 340
Grand Junction, Colorado 81501

ABSTRACT

Pillar design in oil shale by the induced horizontal stress method is based on in-situ stress determinations of pillars before and during failure, on computer analysis incorporating site specific rock properties, and on the pre-mining stress field. An empirical strength equation which relates vertical and horizontal stresses at failure was developed from stress determinations through the center of 60-ft cube pillars. Induced horizontal stresses within the pillars are then evaluated for different width-to-height ratios by simple finite element analysis. Design curves are developed relating pillar stresses and strength with pillar widths and extraction ratios.

The induced horizontal stress method, which is based on the in-situ strength of large pillars, has been used for planning and resource recovery evaluations throughout the Piceance Creek Basin.

INTRODUCTION

Design of mine pillars is performed by empirical methods because of difficulties in assessing and quantifying the in-situ rock strength of large pillars. Pillar design methods have been developed mostly from coal mining experience where many years of room and pillar mining provide a good background for linking experience and theory, and field and laboratory work.

Pillar strengths can be determined essentially by two methods: the width-to-height (W/H) ratio, and the confined core methods. In the first method, described extensively in the literature (1, 2, 3, 4, 5), the strength is related to the pillar width, height, and the laboratory unconfined strength. In the confined core method, the strength is obtained by using a Mohr-Coulomb formulation based on laboratory triaxial strength values and an assumption of a failed outer zone confining an unfailed core (6). Applications of both methods to oil shale have been proposed and are described in the literature (7, 8).

This paper describes another empirical design technique, the induced horizontal stress method, developed for oil shale. This method is based (1) on strength criteria obtained by stress determinations in 60-ft cube pillars performed before and during failure; and (2) on field calibrated computer analysis to project the induced horizontal stresses and strength to locations with different material properties and stress fields. Basic pillar strength criteria was developed at the Colony Pilot Mine and has been described in previous publications (9, 10, 11). This experimental mine is located in the Colony property owned by Exxon Company, the operator, and Tosco Corporation.

GEOLOGIC STRUCTURE OF THE PICEANCE CREEK BASIN

The Piceance Creek Basin contains about 80 percent of the oil shale resources of the Green River Formation; this amounts to about 1200 billion barrels of petroleum equivalent with 600 billion barrels occurring in material with a grade of 25 gal/ton or more. Oil shale is an economic term used for marlstones with a recoverable kerogen content of more than 5 to 10 gal/ton.

Most of the oil shales of economic interest occur in the Parachute Creek Member of the Green River Formation. In this member, the oil shale is divided into rich zones designated R2 through R6, Mahogany and upper oil shale separated by leaner zones designated L2 through L5, A- and B-grooves. Most of the experimental mining operations have been conducted in the Mahogany zone because it is shallower and contains nearly 30 percent of the basin's resource.

Wet sediment deformation features resulting from lake bottom sediment slumping are common through most of the oil shale intervals,

and range from simple pinching-out of thin beds to folding with faults. Folds are broad with northwesterly trending axes. A number of normal faults have been mapped in the central basin; these all strike northwesterly, approximately parallel to the fold axes. Numerous joints occur through the oil shale with two dominant trends: northwest to west-northwest, and northeast to north-northeast.

Locally, well defined systems of joints and bedding planes are present and control the rock mass quality. Joint inclinations may vary from vertical to 45^{o} and more with spacings from a few inches to 10 or more feet. These variations, together with variations in bedding thicknesses, affect rock quality. Generally the rock quality in the richer zones is better than in the leaner zones. For example, rock quality in the mining interval in the Mahogany zone may vary from fair to very good while in the B-groove it may decrease to very poor. These large variations make the assessment of rock quality a very necessary part of every geotechnical program. During the last four years, work has been performed in applying rock mass quality classification systems to oil shale but none of these studies have yet been published.

MECHANICAL PROPERTIES

The mechanical properties of oil shale are greatly dependent on grade as shown by numerous laboratory tests. This dependency can better be described by a series of regression curves of test results relating grade (modified Fischer assay) and various mechanical properties. Figures 1 to 5 show the curves relating grade with density, unconfined compressive strength, Young's modulus, Poisson's ratio, angle of internal friction, and cohesion. Correlations between grade and density are excellent, and quite good with unconfined compressive strength and Young's modulus. Correlations with Poisson's ratio are poor to fair. There is little published data on grade correlations with the angle of internal friction and cohesion because of the smaller number of triaxial tests performed as compared to uniaxial tests. The available data indicates good correlations with the angle of internal friction, and poor correlations with cohesion. There is little or no correlation between grade and the tensile strength obtained from Brazilian tests.

IN-SITU STRENGTH CRITERIA

The pillar strength information used in developing the induced horizontal stress method of pillar design was based on overcoring stress determinations made in pillars before and during failure. The term failure is used here to describe the unloading that occurs when the ultimate load capacity of a pillar is reached. During failure, stresses are transferred to adjacent unfailed pillars or unmined ground. In most cases, failure at the Colony Mine has occurred in a slow, stable manner without extensive pillar spalling or fracturing. Only two pillars out of nine spalled extensively. No complete pillar collapse has occurred. Failure in the case of the two more extensive fractured pillars occurred over a period of a few months, and in the other pillars over a period of years.

Pillar stress determinations were made through the center at mid-pillar height. Stress profiles obtained from these measurements have been published in previous papers (10, 11). Average vertical ($\bar{\sigma}_v$) and horizontal stresses ($\bar{\sigma}_h$) were obtained by dividing the area under the stress profiles by the length overcored. These stresses were then used to find a relation between the maximum shear stress $(\bar{\sigma}_v - \bar{\sigma}_h)/2$, and the normal stress $(\bar{\sigma}_v + \bar{\sigma}_h)/2$ at mid-pillar height. Figure 6 shows the best fit curve through this data which is represented by the equation:

$$\tau_{max} = A(\sigma_n)^a \qquad (1)$$

where: τ_{max} = maximum shear stress $(\bar{\sigma}_v - \bar{\sigma}_h)/2$, (psi)

σ_n = normal stress $(\bar{\sigma}_v + \bar{\sigma}_h)/2$, (psi)

A = 7, constant

a = 0.7, constant

Each point in Figure 6 pertains to a set of stress determinations in one pillar. A plan view of the mine with the pillar locations is also shown. Pillar failure is shown by the progressive decrease in stress. Equation (1) represents an in-situ Mohr envelope for the

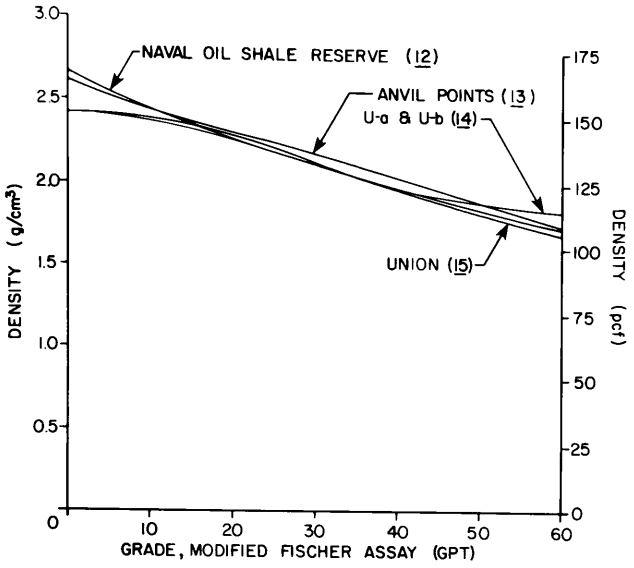

FIGURE 1 – GRADE-DENSITY CORRELATIONS

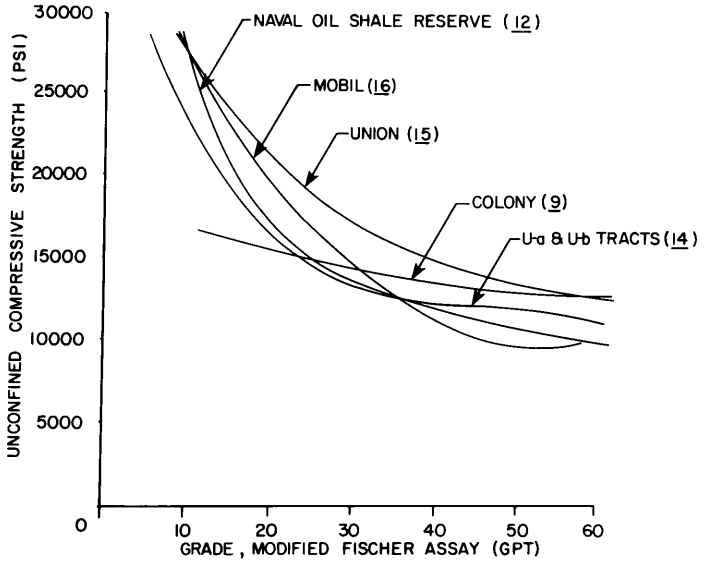

FIGURE 2 – GRADE-UNCONFINED COMPRESSIVE STRENGTH CORRELATIONS

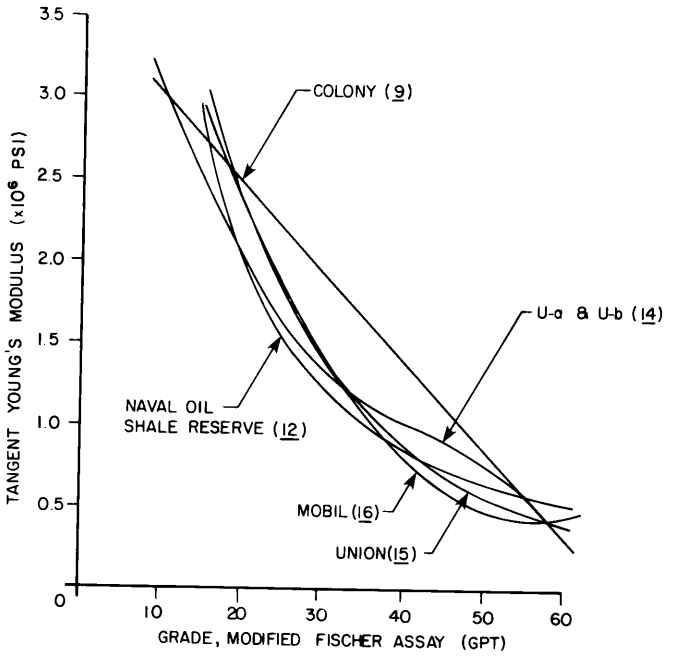

FIGURE 3 – GRADE-YOUNG'S MODULUS CORRELATIONS

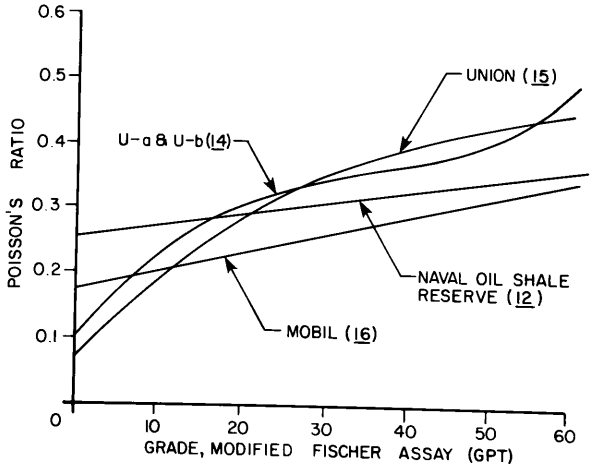

FIGURE 4 – GRADE-POISSON'S RATIO CORRELATIONS

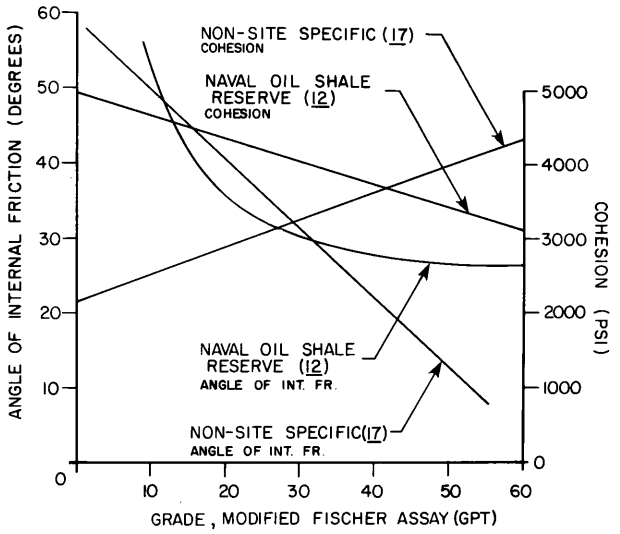

FIGURE 5 — GRADE - ANGLE OF INTERNAL FRICTION CORRELATIONS, AND GRADE-COHESION CORRELATIONS

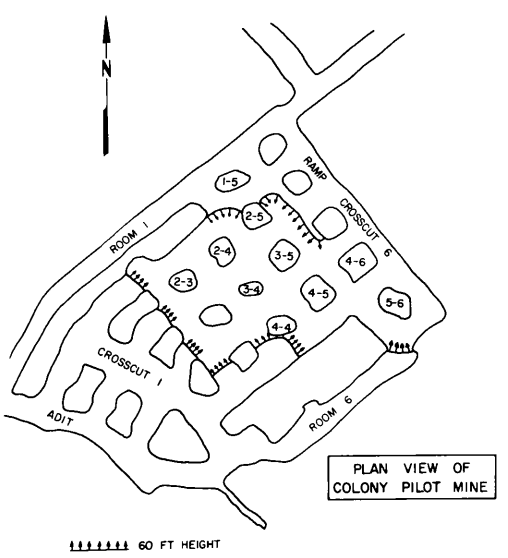

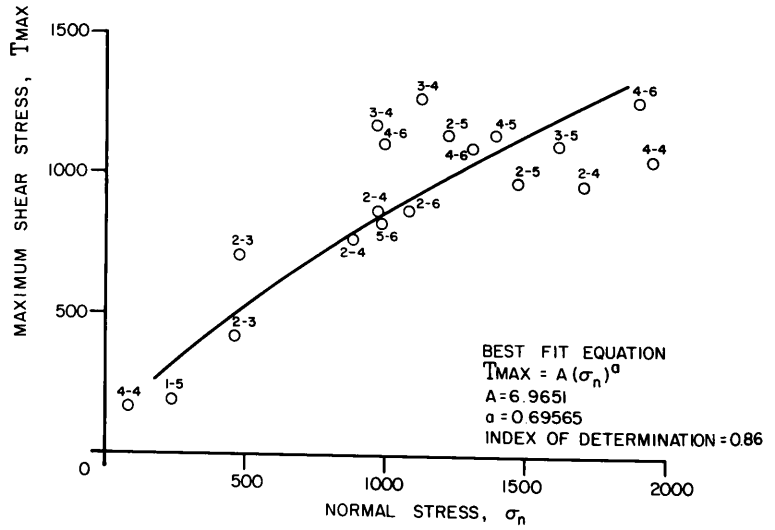

FIGURE 6 — RELATION BETWEEN IN-SITU MAXIMUM SHEAR STRESSES AND NORMAL STRESSES AT MID-PILLAR HEIGHT

60-ft cube pillars and it was used to develop a curve relating the average vertical and horizontal pillar stress at failure (Figure 7). Field measurements indicated that pillar failure began at 3000 to 3250 psi vertical stress and 500 to 700 psi horizontal stress. Significant fracturing was observed only in the more extensively failed pillars, and occurred as a result of both vertical tensile cracks and movement along existing joints (9). In this relatively slow pillar failure there seems to be little or no difference between peak and residual joint strength often observed in laboratory testing.

An equation relating pillar strength, horizontal stresses, and unconfined compressive strength was derived from the compressive region (positive stresses) of Figure 7 with the form:

$$\frac{\bar{\sigma}_v F_s}{\bar{\sigma}} = 1 + B \left(\frac{\sigma_h}{\bar{\sigma}_o}\right)^b \qquad (2)$$

where: $\bar{\sigma}_v$ = pillar strength or average vertical stress at failure, (psi)

F_s = factor of safety

$\bar{\sigma}_o$ = pillar strength at zero horizontal stress = 1300 psi

$\bar{\sigma}_h$ = average horizontal pillar stress (psi)

B = constant = 3.2

b = constant = 0.82

Equation (2) can be used to calculate pillar strength but its application requires that the horizontal stresses for a given pillar size and shape be known.

The curved Mohr envelope shown in Figure 7 can be approximated by a straight line. The slope of this line can be related to the angle of internal friction, $\emptyset$. The calculated in-situ $\emptyset$ is 26.5^o and is very close to the laboratory values for the same 30 to 40 gal/ton grade interval shown in Figure 5. This similarity suggests that laboratory triaxial tests may provide a good basis for calculating in-situ Mohr gradients of non-failed pillars.

The unconfined compressive strength between laboratory and in-situ are very different, but may be related by the following equation:

$$\bar{\sigma}_o = \sigma_{ol} \left(\frac{V_1}{V_i}\right)^{\alpha} \qquad (3)$$

where: $\bar{\sigma}_o$ = in-situ unconfined compressive strength

σ_{ol} = laboratory compressive strength

V_i = in-situ volume of pillar

V_1 = volume of laboratory specimen

α = volume reduction coefficient

Equation (3) expresses the reduction in strength that occurs with an increase of volume of rock. This effect is due to larger rock volumes containing proportionally more flaws or geologic discontinuities than small rock volumes. For design purposes and a given rock type, there is a certain volume above which the strength reduction is no longer significant. This volume of rock must be sufficiently large to contain enough geologic discontinuities to be representative of an in-situ pillar. The key element to obtain the in-situ unconfined strengths is the volume reduction coefficient, α. For the mining interval in the Mahogany zone oil shale, a value of 0.08 has been proposed (7). However, there is evidence to suggest that rock quality, specifically the combined effect of intact rock and geologic discontinuities, influences α. For example, coal having low strength and quality has an α value of 0.12 (18), while hard, good quality quartzite has an α value of 0.06 (19, 20). As applied to oil shale, α should be increased if, for example, the rock quality is significantly lower than that observed at the Colony Pilot Mine. The effect would be to reduce $\bar{\sigma}_o$ in equation (2).

The factor of safety used in equation (2) has a significant impact on the function of the pillars. For example, factors of 0.8 to 1.0 may be appropriate for yielding pillar systems, safety factors of 1.2 to 1.3 for full overburden support systems, and safety factors of 1.4 to 1.6 for barriers and pillars in main accessways.

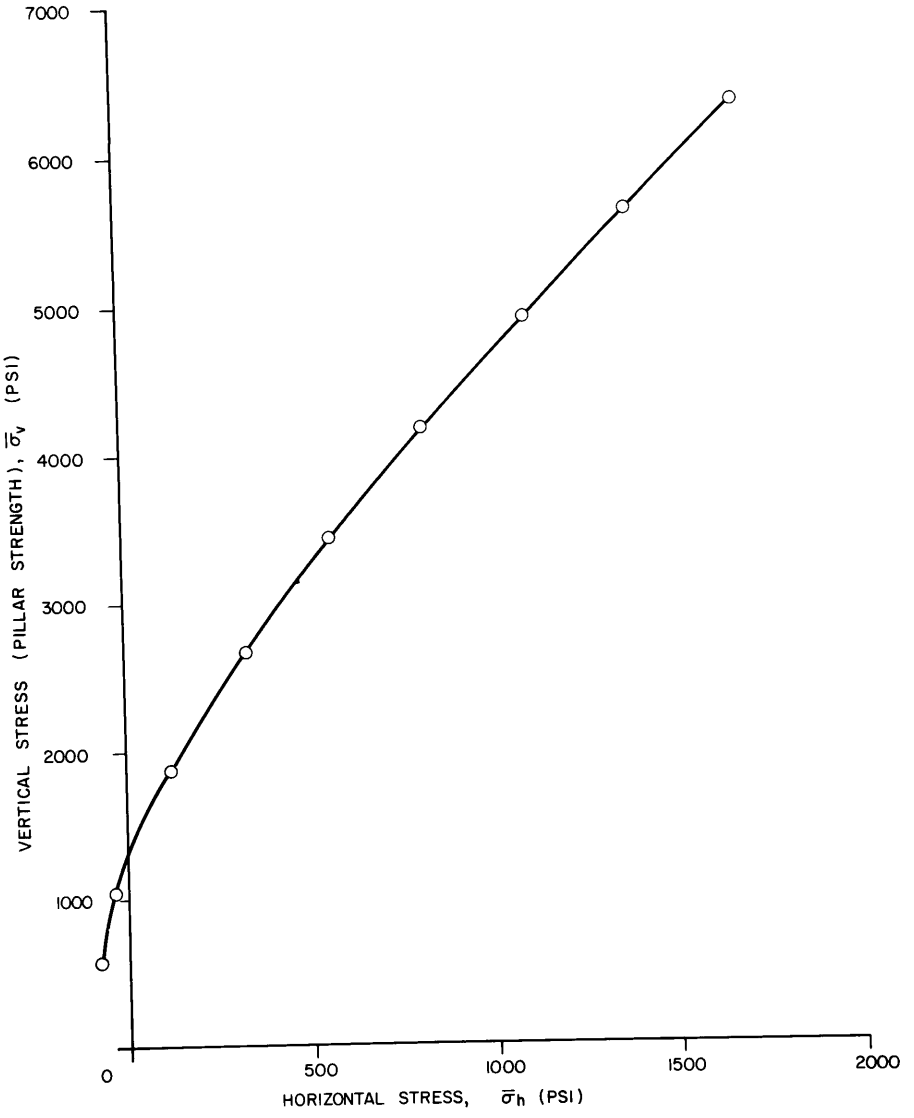

FIGURE 7 – RELATION BETWEEN AVERAGE VERTICAL AND HORIZONTAL STRESSES AT FAILURE, MID-PILLAR HEIGHT

INDUCED HORIZONTAL STRESSES

The horizontal stresses in the pillar increase with the vertical pillar load to the point of failure. Evaluation of induced horizontal stresses is made by a simple finite element analysis which models the average stresses developed at mid-pillar height. Figure 8 shows a typical two-dimensional model. To minimize the number of computer runs while still taking into consideration a number of various depths and stress fields, the induced horizontal stresses in square pillars were expressed by the following equation:

$$\bar{\sigma}_{hp} = [(\sigma_{hi})\ (F_1)] + [(\bar{\sigma}_{vp} - \sigma_{vi})\ (F_2)] \qquad (4)$$

where: $\bar{\sigma}_{hp}$ = average horizontal stresses at mid-pillar height, (psi)

σ_{hi} = initial or pre-mining horizontal stress, (psi)

$\bar{\sigma}_{vp}$ = average vertical stress at mid-pillar height, (psi)

σ_{vi} = initial or pre-mining vertical stress (psi)

F_1, F_2 = factors dependent on pillar shapes and material properties.

Factors F_1 and F_2 depend on the pillar width-to-height ratio and can be determined by two finite element analyses incorporating site specific properties. For very slender pillars, both factors tend to zero; for very squat pillars, F_1 will tend to 1 and F_2 to $\nu/(1 - \nu)$, where ν is the Poisson's ratio. Figure 9 shows typical curves relating F_1 and F_2 to the width-to-height ratio. The rock properties used in the model of Figure 8 were obtained from an evaluation of oil shale grade and laboratory test results. In this particular example, seven horizons with different properties were used in assembling the numerical model.

Equation (3) can be solved by using the graphs of Figure 9 and from an estimate of the pre-mining stress field. A series of straight lines can be calculated for various width-to-height ratios and stress fields. The pillar strength is obtained from the intersection of these lines and the strength curve obtained from solving equation (2). Figure 10 shows the results for a hypothetical case at a depth of 1000 ft with a pre-mining vertical-to-horizontal stress field ratio of 1.0. A vertical stress gradient of 1 psi/ft depth and a safety factor of 1.4 were assumed.

An empirical equation relating strength and pillar width can be obtained for a given property by correlating $\bar{\sigma}_v/\bar{\sigma}_h$ to W/H, the point of intersection of the curves in Figure 10, for various depths. For practical purposes, the error introduced by combining various depths in the same relation is negligible. Once the room spans and mining heights are determined, the pillar strength-width curve can be used to obtain the pillar sizes and extraction ratios. Figure 11 shows a simple example for an oil shale property with a depth range of 600 to 1000 ft, 50-ft wide by 50-ft high rooms, and a hydrostatic stress field. The vertical pillar stresses were obtained by using the tributary area load expressed as:

$$\bar{\sigma}_{vp} = \sigma_{vi}\ \left(\frac{W+S}{W}\right)^2 \qquad (5)$$

and the extraction ratio by using equation:

$$R = 1 - \left(\frac{W}{W+S}\right)^2 \qquad (6)$$

where in equation (4) and (5):

$\bar{\sigma}_{vp}$ = average vertical stress

σ_{vi} = pre-mining vertical stress

R = extraction ratio

W = pillar width

S = room span.

In Figure 11, the pillar widths were obtained at the intersection of the strength and stress curves, and the extraction ratios from the projection of these intersections to the extraction ratio curve.

The induced horizontal stress method has been used for a number of oil shale properties within the Piceance Creek and Uinta Basins. In some of these projects, it has been compared to the width-to-height and confined core methods. Figure 12 shows a comparison of the three methods. The induced horizontal stress method generally gives lower strength values for slender pillars and higher values for pillars with a width-to-height ratio above 1.75.

Although square pillars were used in the examples given in this paper, the method is applicable to rectangular pillars. In this

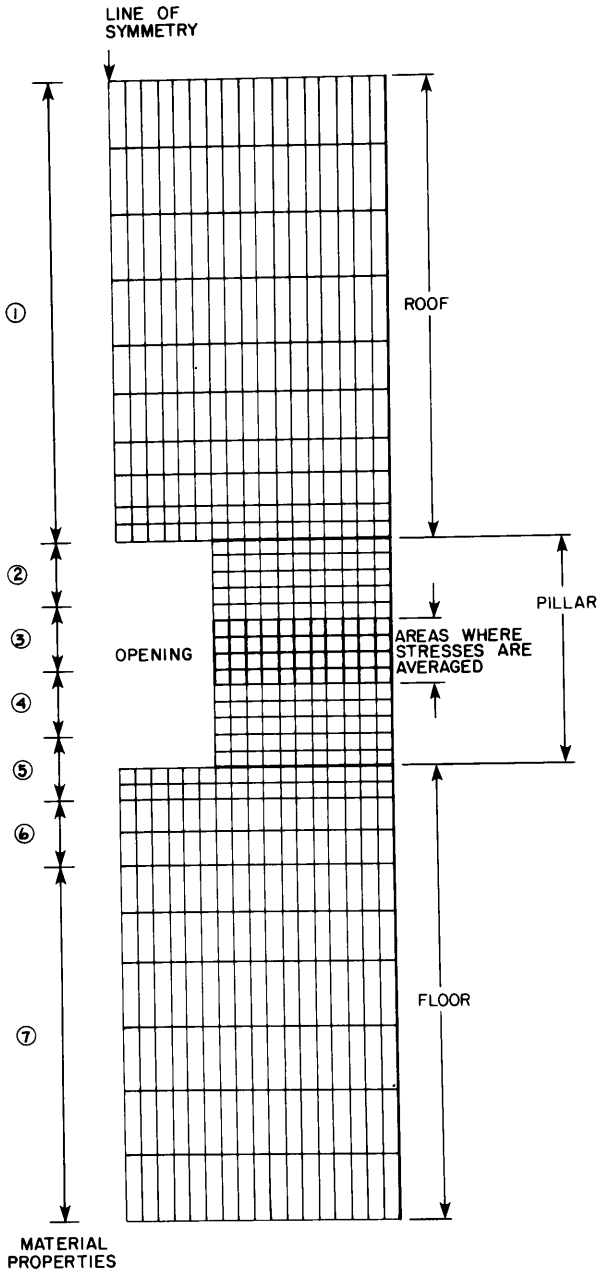

FIGURE 8 - FINITE ELEMENT MODEL

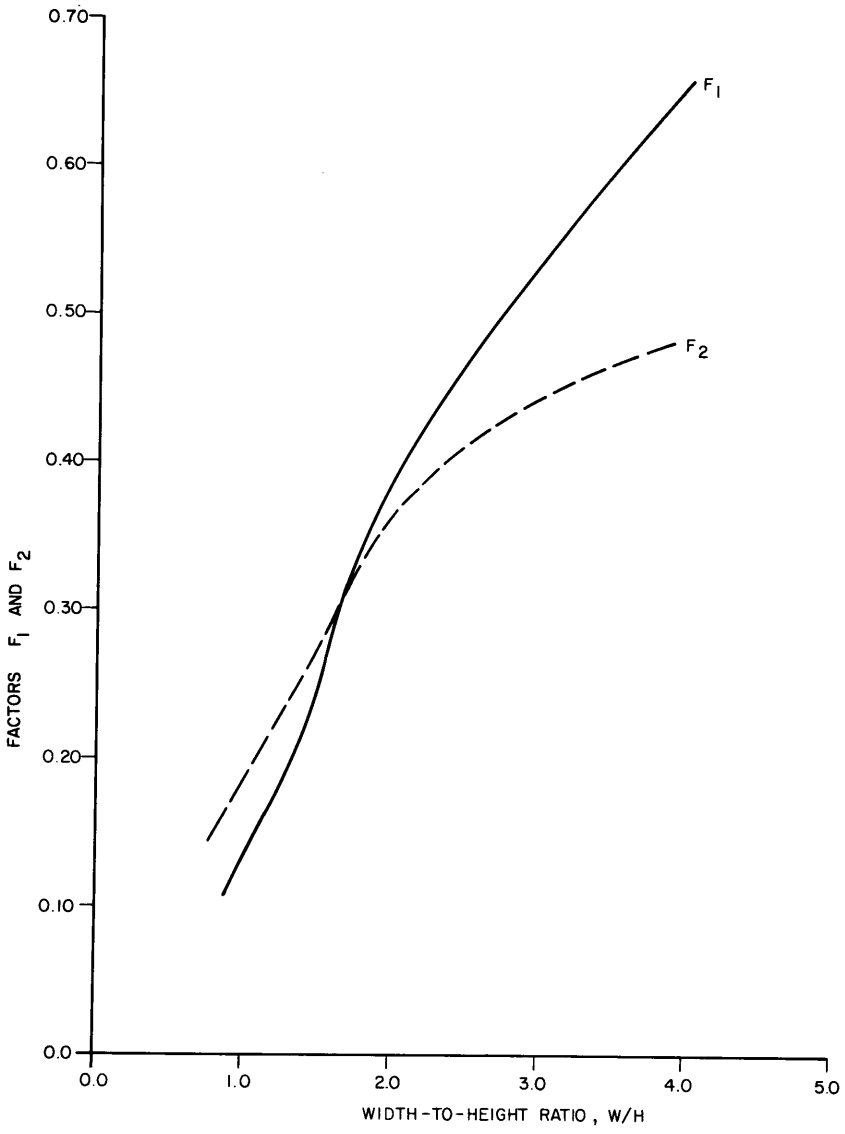

FIGURE 9 – EXAMPLE SHOWING RELATION BETWEEN F_1 AND F_2 AND W/H RATIO

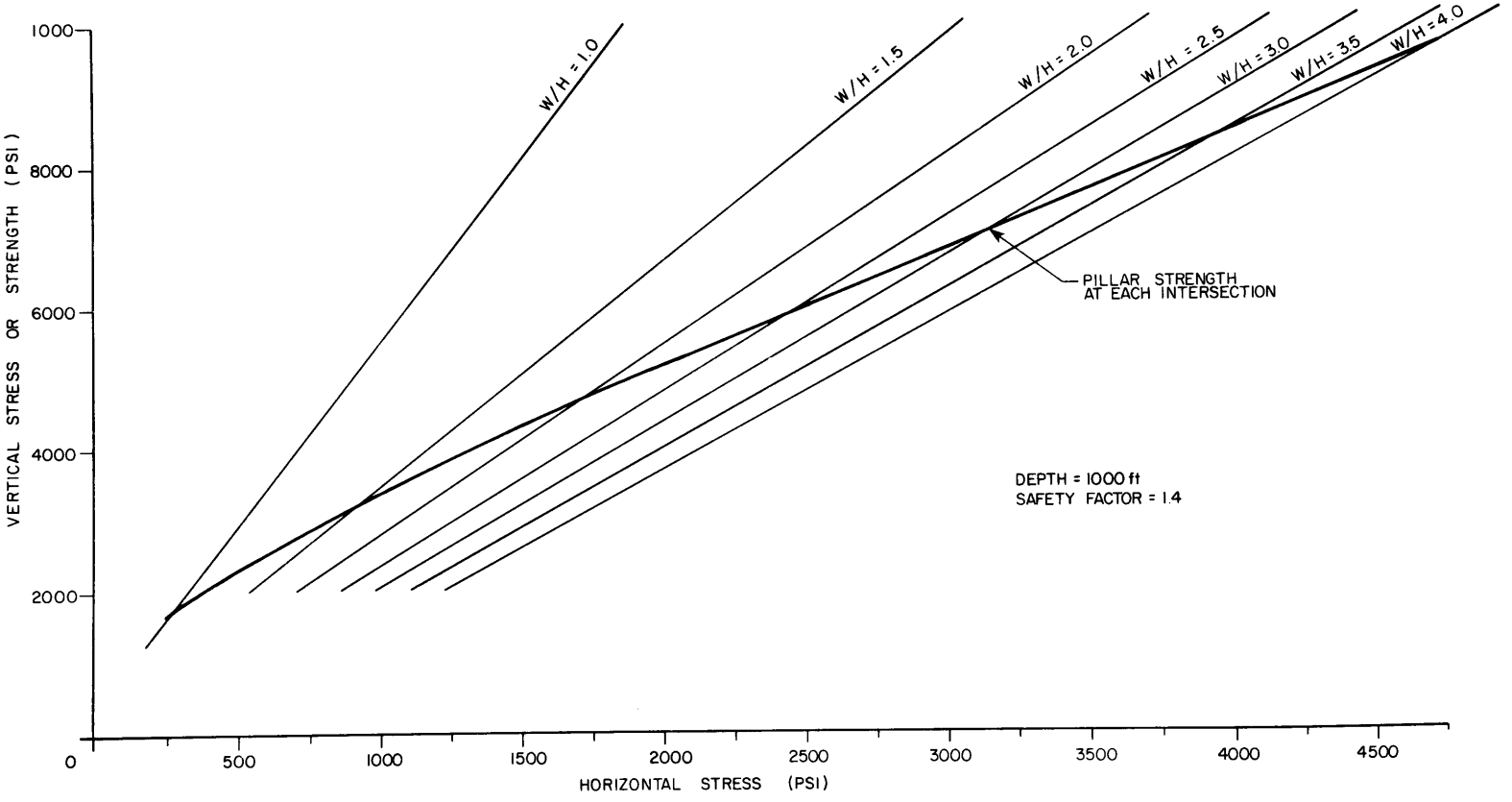

FIGURE 10 – STRENGTH DETERMINATIONS FOR VARIOUS PILLAR WIDTH-TO-HEIGHT RATIOS

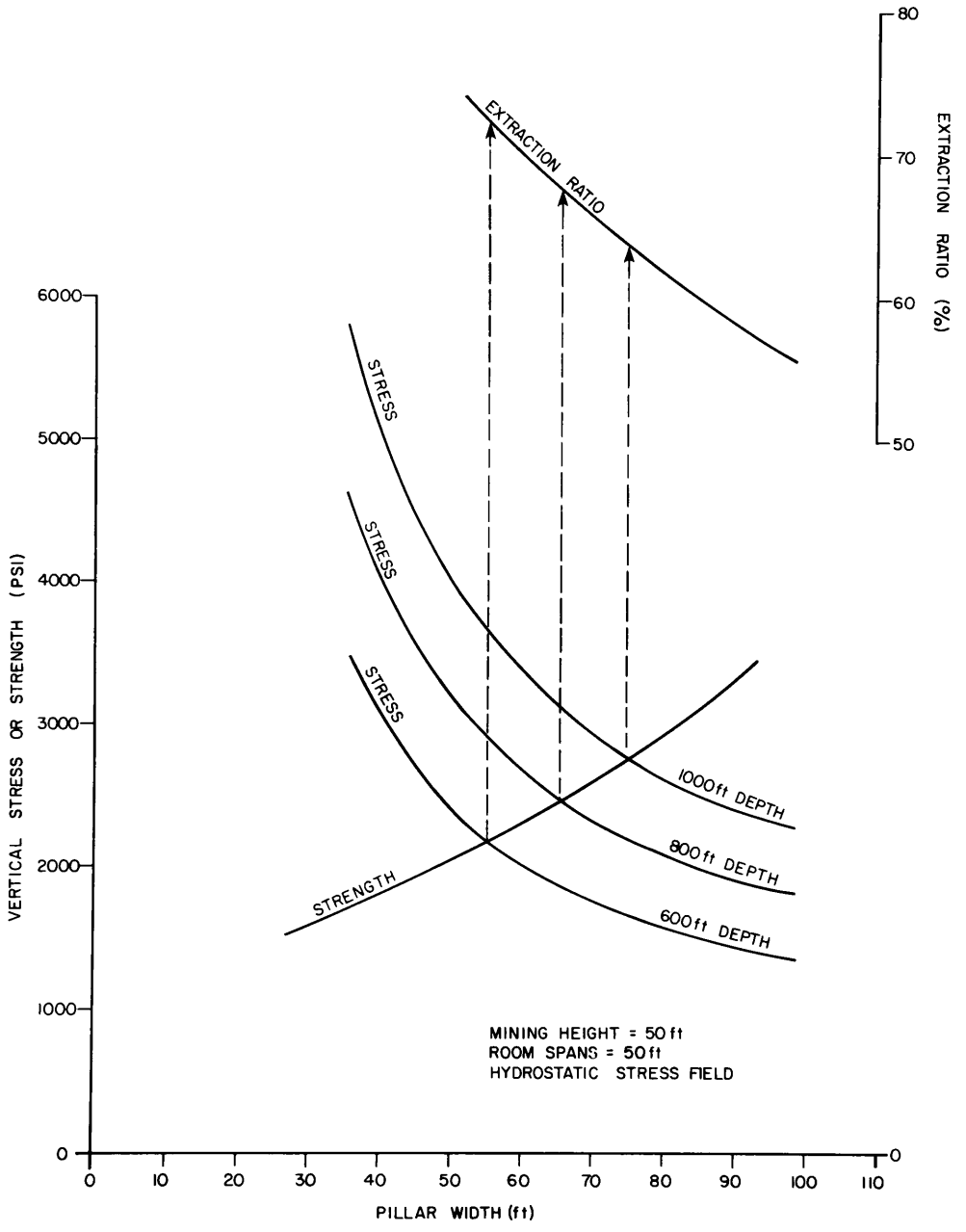

FIGURE 11 – EXAMPLE SHOWING RELATION BETWEEN PILLAR STRESS, STRENGTH AND WIDTH, AND EXTRACTION RATIO

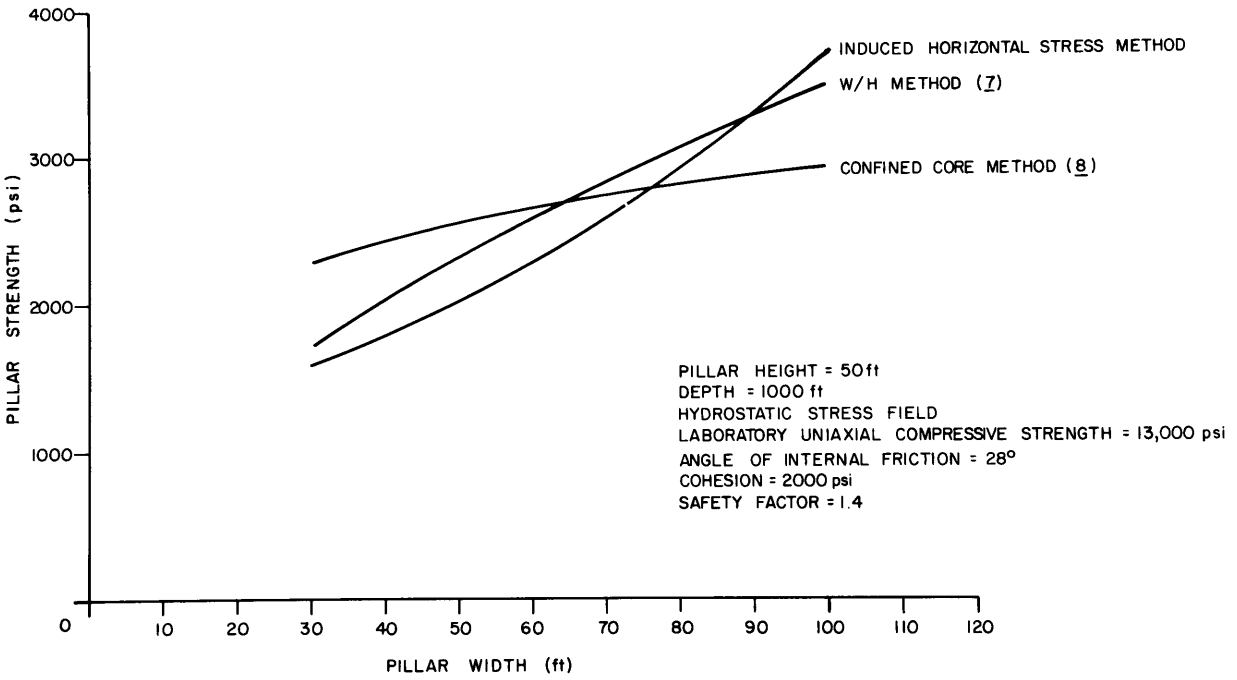

FIGURE 12 - COMPARISON OF PILLAR STRENGTH DESIGN METHODS

case, the pillar strength is controlled by the smaller pillar dimension.

CONCLUSIONS

The induced horizontal stress method of pillar design is based on strength criteria developed by monitoring stable pillar failure in an experimental oil shale mine. Overcoring measurements at mid-pillar height made before and during failure provided data to develop an empirical equation relating the average vertical and horizontal stress at failure. Simple computer analyses were then made to obtain the induced horizontal stresses for various pillar dimensions, depths, and stress field. These calculated induced horizontal stresses are used to obtain pillar strength and sizes.

Comparison with the other empirical design methods show relatively close agreement with the induced horizontal stress method giving lower strengths for slender pillars and higher strengths for squatter pillars. The higher increase in strength in the squatter pillars reflects the mobilization of strength caused by the induced horizontal stresses associated with higher vertical loads.

REFERENCES

1. Salamon, M.D.G., and Munro, A.H., 1967. A Study of the Strength of Coal Pillars, Journal of the South African Institute of Min. Metall., Vol. 68, No. 2, pp. 55-67.

2. Greenwald, H.P., Howarth, H.C., and Hartmann, I., 1939. Experiments on the Strength of Small Pillars of Coal in the Attsburgh Bed, Tech. Rept. No. 605, U.S. Bureau of Mines.

3. Holland, C.T., 1964. The Strength of Coal in Mine Pillars, Proceedings, 6th Symposium on Rock Mechanics, Rolla, Missouri, pp. 450-456.

4. Bieniawski, Z.T., and Van Heerden, W.L., 1975. The Significance of In-Situ Tests on Large Rock Specimens, International Journal of Rock Mechanics and Mining Sciences and Geomechanics Abstracts, Vol. 12.

5. Hustrulid, W.H., 1976. A Review of Coal Pillar Strength Formulas, Rock Mechanics, Vol. 8, pp. 115-145.

6. Wilson, A.H., 1972. Research Into the Determination of Pillar Size, Pt. 1, A Hypothesis Concerning Pillar Stability, Mining Engineer, V. 131, No. 141, pp. 409-417.

7. Hardy, M.P., and Agapito, J.F.T., 1975. Pillar Design in Underground Oil Shale Mines, Proc. 16th Symposium on Rock Mechanics, Minneapolis, S.L. Crouch and C. Fairhurst, eds., pp. 325-335.

8. Abel, J.F., and Hoskins, W.N., 1976. Confined Core Pillar Design for Colorado Oil Shale, 9th Oil Shale Symposium, Colorado School of Mines.

9. Agapito, J.F.T., 1972. Pillar Design in Competent Bedded Formations, Colorado School of Mines, Ph.D. Thesis, May.

10. Agapito, J.F.T., 1974. Rock Mechanics Applications to the Design of Oil Shale Pillars, SME Reprint 74-AIME-26.

11. Agapito, J.F.T., and Page, J.B., 1976. A Case Study of Long-Term Stability in the Colony Oil Shale Mine, Piceance Creek Basin, Colorado, Proceedings, 17th U.S. Symposium on Rock Mechanics, August.

12. Dolinar, D.R., Horino, F.G., and Hooker, V.E., 1979. Mechanical Properties of Oil Shale and Overlying Strata, Naval Oil Shale Reserve, Anvil Points, Colorado, USBM Denver Research Center Progress Report 10024, August.

13. East, J.F., and Gardner, E.D., 1964. Oil Shale Mining, Rifle, Colorado, 1944-56, USBM Bulletin 611.

14. Horino, F.G., and Hooker, V.E., 1975a. The Mechanical Properties of Oil Shale, White River Oil Shale Corp., Uintah County, Utah. USBM Denver Min. Res. Center Progress Report 10014 (U-a and U-b Tracts).

15. Horino, F.G., and Hooker, V.E., 1975b. The Mechanical Properties of Oil Shale, Union Oil Company of California, Garfield County, Colorado, USBM Denver Min. Res. Center Progress Report 10015.

16. Sellers, J.B., Haworth, G.R., and Zambas, P.G., 1972. Rock Mechanics Research on Oil Shale Mining, SME/AIME Transactions, V. 252, No. 2, June.

17. Cameron Engineers, 1975. A Technical and Economic Study of Candidate Underground Mining Systems for Deep, Thick Oil Shale Deposits, Phase I Report, USBM Contract Report S0241074, July.

18. Hoek, E., and Brown, E.T., 1980. Underground Excavations in Rock, Institution of Min. Metall., London, 527 pp.

19. Coates, D.F., Bielenstein, H.V., and Hedley, D.F.G., 1973. A Rock Mechanics Case History of Elliot Lake, Canadian J. Earth Sciences, Vol. 10, No. 7, pp. 1023-1058.

20. Kostak, B., and Bielenstein, H.V., 1971. Strength Distribution in Hard Rock, Int. J. Rock Mech. Min. Sci., Vol. 8, pp. 501-521.